

Path integral loop representation of 2+1 lattice non-Abelian gauge theories

J. M. Aroca

Departament de Matemàtiques, Universitat Politècnica de Catalunya, Jordi Girona 1 i 3, Mod C-3 Campus Nord, 08034 Barcelona, Spain

Hugo Fort and Rodolfo Gambini

Instituto de Física, Facultad de Ciencias, Tristan Narvaia 1674, 11200 Montevideo, Uruguay

(Received 20 January 1998; published 10 July 1998)

A gauge invariant Hamiltonian representation for $SU(2)$ in terms of a spin network basis is introduced. The vectors of the spin network basis are independent and the electric part of the Hamiltonian is diagonal in this representation. The corresponding path integral for $SU(2)$ lattice gauge theory is expressed as a sum over colored surfaces, i.e., only involving the j_p attached to the lattice plaquettes. These surfaces may be interpreted as the world sheets of the spin networks in 2+1 dimensions; this can be accomplished by working in a lattice dual to a tetrahedral lattice constructed on a face centered cubic Bravais lattice. On such a lattice, the integral of gauge variables over boundaries or singular lines — which now always bound three colored surfaces — only contributes when four singular lines intersect at one vertex and can be explicitly computed producing a 6-j or Racah symbol. We performed a strong coupling expansion for the free energy. The convergence of the series expansions is quite different from the series expansions which were performed in ordinary cubic lattices. Our series seems to be more consistent with the expected linear behavior in the weak coupling limit. Finally, we discuss the connection in the naive continuum limit between this action and that of the B-F topological field theory and also with the pure gravity action. [S0556-2821(98)05914-1]

PACS number(s): 11.15.Ha, 04.60.Nc

I. INTRODUCTION

The loop approach to Abelian quantum gauge theories was introduced in the early 1980s [1]. Later it was generalized to non-Abelian Yang-Mills gauge theory [2]. This Hamiltonian method allows one to formulate gauge theories in terms of their natural physical excitations: the loops. The original aim of this general description of gauge theories was to avoid gauge redundancy working directly in the space of the gauge invariant excitations. However, soon it was realized that the loop formalism goes far beyond a simple gauge invariant description. The introduction by Ashtekar [3] of a new set of variables that cast general relativity in the same language as gauge theories allowed one to apply loop techniques as a natural nonperturbative description of Einstein's theory. In particular, the loop representation appeared as the most appealing application of the loop techniques to this problem [4].

Recently a Lagrangian approach in terms of loops has been developed for the $U(1)$ model [5], and generalized to include matter fields [6]. The resulting action is proportional to the quadratic area of the loop world sheet. This allows for Monte Carlo simulations in a more efficient way than by using the gauge potentials as variables. While in the Abelian case the usual Hamiltonian in the loop representation can be deduced from the loop action by means of the transfer matrix analysis, the relation between the two approaches is more obscure in the non-Abelian case. In fact, the type of surfaces that appear in the Lagrangian loop formulation suggest that the pass to the Hamiltonian can be made simpler if we take a representation different from the loop representation but one that shares important features like the use of gauge invariant geometrical objects known as "spin networks" [7]. A spin

network basis may be obtained by considering linear combinations of loops. While the loop basis is overcomplete and therefore is constrained by a set of identities known as the Mandelstam identities, the vectors of spin network basis are independent. Furthermore the electric part of the Yang-Mills Hamiltonian is diagonal in spin network space.

A path integral formulation of $SU(2)$ gauge theories in terms of the world sheets swept out by spin networks has been developed in [8] and [9]. The world sheets are branched, colored surfaces. Such surfaces were introduced in the 1970s [10] in the context of strong coupling calculations in Yang-Mills theory. The starting point was a character expansion of the Wilson action. This expansion leads after integration on the link variables to a sum of contributions proportional to the coupling constant raised to a power proportional to the area of closed colored surfaces. Each colored surface corresponds to a diagram having a certain number of plaquettes. In the usual hypercubic lattice formulation [10] the higher order terms in the expansion become extremely complicated, discouraging attempts to reformulate gauge theories directly in terms of the colored surfaces. The main difficulty lies in the computation of certain group theoretic factors for each surface. Nevertheless it is possible to reformulate gauge theories in terms of the surfaces along these lines [8].

In the present paper we show that most of the complications of the group theoretic factors can be avoided by working on a special class of noncubic lattices, namely the duals to tetrahedral lattices. This leads to an easy calculation of the action of spin network world sheets, and also simplifies the explicit calculation of strong coupling expansions.

The loop actions of the Abelian gauge theories are written in terms of the surfaces swept by the time evolution of the

loops. The explicit form of the loop actions for lattice non-Abelian gauge theories is known to be related to colored surfaces [8,9,11]. They are related to the world sheet swept by the evolution in time of the spin networks. However, a complete Lagrangian lattice formulation associated with the spin network representation was not available up to now.

In Sec. II we discuss the spin network Hamiltonian approach to Yang-Mills theory. In Sec. III we study the character expansion of the Wilson action and we show why the group factors do not allow to get a closed form for the action in terms of colored surfaces. In Sec. IV we show that these factors may be simply computed in a tetrahedral lattice where the Wilson action and the heat kernel action take a very simple form. In Sec. V we apply this action to perform a strong coupling expansion for the heat kernel version of the theory and we compute the free energy density f and the average plaquette P . Finally, in Sec. VI we conclude with some comments on further developments.

II. SPIN NETWORK REPRESENTATION

We consider the pure gauge theory with gauge group G semisimple and compact [$G=U(1)$ or $SU(n)$]. We start with the Hilbert space $\mathcal{H}=\otimes_l \mathcal{H}_l$ where $\mathcal{H}_l=L_2(G)$ and l denote the links of the lattice. On every link l we take the ‘‘position’’ basis $|U_l\rangle$ labeled by the fundamental representation matrices $U_l \in G$. A basis of \mathcal{H} is given by the vectors $|U\rangle=\otimes_l |U_l\rangle$. Links are oriented and $U_{\bar{l}}=U_l^{-1}$.

A gauge transformation is specified by a group element V_s on every lattice site s . The state $|U\rangle$ is transformed into $|U'\rangle$ where $U'_l=V_{s_1} U_l V_{s_2}^{-1}$, s_1 and s_2 being the origin and end of l . The physical states are those that are invariant under gauge transformations and they define the physical Hilbert space \mathcal{H}_{phys} .

The position and momentum operators \hat{U}_l, \hat{E}_l^a are defined

$$\hat{U}_l |U\rangle = U_l |U\rangle, \quad (1)$$

$$e^{i\theta^a \hat{E}_l^a} |U\rangle = |U'\rangle, \quad (2)$$

where $U'_l = e^{i\theta^a T^a} U_l$, T^a are generators of the group satisfying

$$\text{Tr}(T^a T^b) = \frac{\delta^{ab}}{2}, \quad (3)$$

$$[T^a, T^b] = i c^{abc} T^c. \quad (4)$$

The reference state $|0\rangle = \int dU |U\rangle$ is gauge invariant and permits to express any state $|\psi\rangle = \psi(\hat{U})|0\rangle$. To work in the physical space \mathcal{H}_{phys} we have to find a basis $|\psi_\alpha\rangle$, that is, a collection of appropriate gauge invariant functions $\psi_\alpha(U)$.

One choice is to consider polynomials

$$\prod_l (U_l)_{a_1 b_1} \cdots (U_l)_{a_r b_r} (U_l^{-1})_{c_1 d_1} \cdots (U_l^{-1})_{c_s d_s}. \quad (5)$$

Imposing gauge invariance leads to contraction of indices of incoming and outgoing matrices at every site. The result is the loop representation. That is, states

$$|C_1, C_2, \dots, C_M\rangle = W(C_1)W(C_2)\cdots W(C_M)|0\rangle, \quad (6)$$

where C_i are closed loops and

$$W(C) = \text{Tr} \prod_{l \in C} U_l. \quad (7)$$

These states generate \mathcal{H}_{phys} but they are not independent. They satisfy the so called Mandelstam constraints which for $SU(2)$ read

$$W(C_1)W(C_2) = W(C_1 C_2) + W(C_1 \bar{C}_2), \quad (8)$$

for every two loops C_1, C_2 with the same origin.

Instead of Eq. (5) we can consider the states given by functions

$$\prod_l D_{a_l b_l}^{(\mu_l)}(U_l), \quad (9)$$

where μ runs over the irreducible representations of G and $D^{(\mu)}$ are the matrices of these representations. (Links in the trivial representation are not mentioned explicitly.) Looking to a vertex where enter links in the μ_1, \dots, μ_r representations and leave links in the ν_1, \dots, ν_s representations we have functions

$$D_{a_1 b_1}^{(\mu_1)}(U_1) \cdots D_{a_r b_r}^{(\mu_r)}(U_r) D_{c_1 d_1}^{(\nu_1)}(V_1) \cdots D_{c_s d_s}^{(\nu_s)}(V_s) \times (V_r) \lambda_{b_1 \dots b_r c_1 \dots c_s}^{[\mu_1 \dots \mu_r \nu_1 \dots \nu_s]}, \quad (10)$$

where $\lambda[\dots]$ are coefficients that ensure gauge invariance. (We sum over repeated latin indices.) If we perform a gauge transformation with element g at the present site we see that λ must be an invariant tensor

$$\lambda_{a_1 \dots a_r b_1 \dots b_r c_1 \dots c_s}^{[\mu_1 \dots \mu_r \nu_1 \dots \nu_s]} = D_{a_1 b_1}^{(\mu_1)}(g^{-1}) \cdots D_{a_r b_r}^{(\mu_r)}(g^{-1}) \times D_{c_1 d_1}^{(\nu_1)}(g) \cdots D_{c_s d_s}^{(\nu_s)}(g) \times \lambda_{b_1 \dots b_r c_1 \dots c_s}^{[\mu_1 \dots \mu_r \nu_1 \dots \nu_s]}. \quad (11)$$

The λ tensors can be computed from the Clebsh-Gordan (CG) coefficients for the group. The condition for λ being nonzero is that the decompositions of the product of the representations entering and the product of the representations leaving have common terms. The representation defined by these states is called *spin network representation*. The states are represented graphically as oriented paths with branching points where every single line is labeled by a representation of the group (see Fig. 1).

Suppose now that the group is Abelian [$G=U(1)$]. Then the irreducible representations are one-dimensional and have the form $D^{(n)}(U) = U^n$ for $n \in \mathbf{Z}$. So the Eq. (9) states coin-

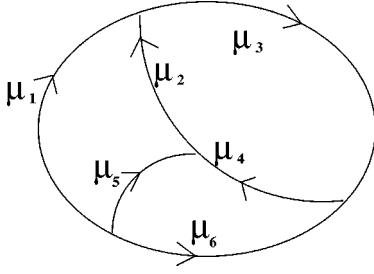


FIG. 1. An example of spin network.

side with the polynomial states (5) and the loop representation and the spin network representation are the same.

For non-Abelian G the two representations are different. It is clear that a site cannot have only one link entering or only one link leaving. The simplest case is one link entering and another link leaving. Both must be in the same representation and the invariant tensor is

$$\lambda \begin{matrix} \mu \\ | \\ a \end{matrix} \begin{matrix} \mu \\ | \\ d \end{matrix} = \delta_{ad}. \quad (12)$$

The effect of this tensor is to multiply the matrices that enter and leave so single lines in the spin network are labeled by a single representation. The case of two links entering a site is forbidden in general but in the case of $SU(2)$ there are invariant tensors like ϵ_{ab} (antisymmetric and $\epsilon_{12}=1$). The effect of these tensors is to reverse one of the lines converging on the site. This is due to the fact that for $SU(2)$ every representation is equivalent to its conjugate.

When three lines meet in a site the condition for the existence of nonzero invariant tensors is that the product of the entering representations contains the trivial representation. In that case the invariant tensor is given by the CG coefficients

$$D_{ab}^{(\mu)}(g)D_{cd}^{(\nu)}(g) = \sum_{\rho} C(\mu a, \nu c | \rho d) D_{de}^{(\rho)}(g) C(\rho e | \mu b, \nu d), \quad (13)$$

which are taken real

$$C(\mu a, \nu b | \rho c) = C(\rho c | \mu a, \nu b). \quad (14)$$

As we consider only simply reducible groups no other independent invariant tensor exists. Then the state corresponding to a trivalent vertex is well encoded in the drawing of the spin network. This is not in general the case for sites where four or more lines meet. The dimension of the space of invariant tensors is the number of times that the product of the entering representations contains the trivial representation. Besides the spin network it must be provided information about which tensors we select on the vertices. This degeneration is not fundamental since these vertices can be thought of as the limiting case when the line connecting two trivalent vertices gets zero length. (See Fig. 2.)

A spin network is denoted $\mathcal{N} = P_1 P_2 \cdots P_M$ where P_i are the single lines. μ_i is the representation carried by line P_i . The spin network states $|\mathcal{N}\rangle$ are independent and orthonormal. A proof using an inner product structure on the state space is given in [7]. Loop states can be expanded in spin

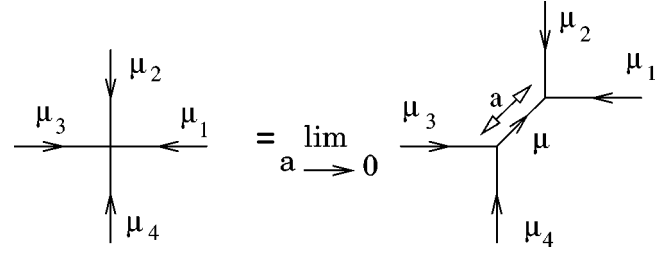


FIG. 2. Four valent vertex as the limiting case of two trivalent vertices.

network terms in a unique way so the Mandelstam constraints disappear when we pass to the spin network representation.

The Hamiltonian operator is

$$H = \frac{g^2}{2} \sum_l \hat{E}_l^2 - \frac{1}{2g^2} \sum_p (W(p) + W(\bar{p})), \quad (15)$$

where g is the coupling constant, l and p are the links and plaquettes of the lattice respectively, and $\hat{E}_l^2 = \hat{E}_l^a \hat{E}_l^a$ and $W(p)$ is given by Eq. (7). The fundamental commutation relations are ($T_a^{(\mu)}$ are the generators of the μ irrep)

$$[\hat{E}_l^a, D^{(\mu)}(\hat{U}_l')] = -T_a^{(\mu)} D^{(\mu)}(\hat{U}_l) \delta_{ll'} + D^{(\mu)}(\hat{U}_l') T_a^{(\mu)} \delta_{\bar{l}l'}, \quad (16)$$

$$[\hat{E}_l^a, \hat{E}_l^b] = i c^{abc} \hat{E}_l^c. \quad (17)$$

We get, for the action of the electric part of the Hamiltonian,

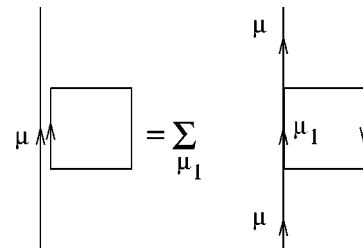
$$\sum_l \hat{E}_l^2 |\mathcal{N}\rangle = L(\mathcal{N}) |\mathcal{N}\rangle, \quad (18)$$

$$L(\mathcal{N}) = \sum_i c^{(\mu_i)} L(P_i), \quad (19)$$

where $L(P_i)$ is the number of links in the line P_i and $c^{(\mu)}$ is the quadratic Casimir number of the representation given by $T_a^{(\mu)} T_a^{(\mu)} = c^{(\mu)} Id$. For example, for $SU(2)$, $c^{(j)} = j(j+1)$.

Then the spin network states, in contrast to the loop states, are always eigenstates of the electric term.

The magnetic part produces deformations of the spin networks both in the geometrical shape and the representations of the lines. This is represented graphically in Fig. 3.


 FIG. 3. Action of the magnetic operator $W(p)$.

To further clarify the relation between loop and spin network states we recall the action of the electric part of the Hamiltonian over a loop state (6)

$$\begin{aligned} \sum_l \hat{E}_l^2 |C_1, C_2, \dots, C_M\rangle &= \left(nL(C_1, C_2, \dots, C_M) - \frac{1}{n} \Lambda(C_1, C_2, \dots, C_M) \right) |C_1, C_2, \dots, C_M\rangle \\ &+ \sum_i \sum_{l, l'} \bar{\delta}_{l, l'} |C_1, \dots, C_{ixy}, C_{iyx}, \dots, C_M\rangle \\ &+ 2 \sum_{i < j} \sum_{l \in C_i} \sum_{l' \in C_j} \bar{\delta}_{l, l'} |C_1, \dots, (C_{ixx} C_{jyy}), \dots, C_M\rangle, \end{aligned} \quad (20)$$

where $L(C_1, C_2, \dots, C_M)$ is the number of links in the set of loops taking account of the multiplicity (single length), and $\Lambda(C_1, C_2, \dots, C_M)$ is the sum of the squares of these multiplicities (quadratic length). $\bar{\delta}_{l, l'}$ is 1 if $l = l'$ and -1 if $\bar{l} = l'$ and x, y are the edges of l .

In Eq. (20) we see that in general the loop states are not eigenstates of the electric operator. The last two sums are geometric interaction terms: fusions where a loop splits into two components and fissions where two loops join in a common link.

Hamiltonian strong coupling expansions on a cubic lattice for SU(2) and SU(3) are given in [12].

III. THE WILSON ACTION IN A CUBIC LATTICE

The path integral for the Wilson action for a general non-Abelian compact gauge group G is given by

$$Z_W = \int [dU_l] \exp \left[\beta \sum_p \text{Re}(\text{Tr } U_p) \right], \quad (21)$$

where the $U_l \in G$ and $U_p = \prod_{l \in p} U_l$.

The analog of the Fourier expansion for the non-Abelian case is the *character* expansion. The characters $\chi_r(U)$ of the irreducible (unitary) representation r of dimension d_r , defined as the traces of these representations, are an orthonormal basis for the *class* functions of the group: i.e. [10],

$$\int dU \chi_r(U) \chi_s^*(U) = \delta_{rs}, \quad (22)$$

$$\sum_r d_r \chi_r(UV^{-1}) = \delta(U, V). \quad (23)$$

In particular, as a useful consequence we have

$$d_r \int dU \chi_s(U) \chi_r(UV^{-1}) = \delta_{rs} \chi_r(V). \quad (24)$$

By means of the character expansion we can express

$$\exp \left\{ \beta \sum_p \text{Re}[\text{Tr } U_p] \right\} = \prod_p \sum_r c_r \chi_r(U_p), \quad (25)$$

with

$$c_r = \int dU \chi_r^*(U) \exp(\beta \text{Tr } U). \quad (26)$$

In the case of $G = \text{SU}(2)$ a direct application of Eq. (26) yields the c_j in terms of modified Bessel functions, and therefore we can express Eq. (21) as

$$\begin{aligned} Z_W &= \int [dU_l] \prod_p \left[\sum_{j_p} 2(2j_p + 1) \frac{I_{2j_p+1}(\beta)}{\beta} \chi_{j_p}(U_p) \right] \\ &= \sum_{\{j_p\}} \prod_p \left[2(2j_p + 1) \frac{I_{2j_p+1}(\beta)}{\beta} \right] \int [dU_l] \prod_p \chi_{j_p}(U_p). \end{aligned} \quad (27)$$

It will be convenient to introduce the following quantities in order to rewrite the path integral Z_W :

$$c_0 = \frac{2I_1(\beta)}{\beta}, \quad (28)$$

$$c_0 \beta_j = \frac{2I_{2j+1}(\beta)}{\beta}. \quad (29)$$

The path integral takes the form

$$Z_W = c_0^N \int \prod_p \left[1 + \sum_{j_p \neq 0} (2j_p + 1) \beta_j \chi_{j_p}(U_p) \right] \prod_l dU_l, \quad (30)$$

where N is the number of plaquettes.

Let us now show how the sum over colored surfaces arise in Z_W . A given subset of plaquettes carrying $j_p \neq 0$ is homeomorphic to a simple surface if any link bounds at most two plaquettes of this subset. The links bounding exactly one plaquette make up the free boundary of this surface. Any configuration can be decomposed as a set of maximal simple surfaces by cutting it along the links bounding more than two plaquettes. In principle, there are two possibilities for the boundary curves: either a free boundary, bounding only one simple surface or a singular branch line along which more than two simple surfaces meet. In fact, relation (22) forbids the existence of free boundaries for nontrivial configurations contributing to the path integral.

The integration over the internal links of the simple surfaces is performed using Eq. (24). Note that the plaquettes of a simple surface component should carry the same group representation. After integrating over all the inner links of the simple components one gets [13] an expression involving only the links of the boundaries:

$$Z_W = c_0^N \sum_{\text{surfaces}} \int \left(\prod_{l \in \partial A} dU_l \right) \times \prod_i \beta_{j_i}^{A_i} (2j_i + 1)^{\epsilon_i} \prod_{\text{boundaries}} \chi_{j_i}[\partial A_i], \quad (31)$$

where ϵ_i is Euler's topological invariant of the surface i with area A_i . Euler's characteristic is explicitly given by

$$\epsilon = n_2 - n_1 + n_0 = 2 - 2g - b, \quad (32)$$

where n_2 is the number of plaquettes, n_1 the number of distinct links bordering these plaquettes and n_0 the number of end points of these links, and g is the genus of the surface and b the number of boundaries.

An important property of the character expansion (27), relevant for strong coupling expansions, is that only a finite number of terms in Eq. (25) contribute to a given order in β . In fact,

$$c_r = O[\beta_r^{\nu_r}], \quad (33)$$

where ν_r is the smallest integer such that $\chi^{\nu_r}(U)$ has a non-vanishing component along $\chi_r(U)$. In the SU(2) case $\nu_j = 2j$.

In [8] and [9] a path integral over colored surfaces is obtained along the lines described here. However, on a cubic lattice the group factors of the surfaces are difficult to compute because with up to four surfaces meeting at singular lines, and up to six singular lines meeting at points, the integral in Eq. (27) can be very complicated, involving recoupling coefficients of up to 12 j 's. That is why these group factors have been only perturbatively computed for the diagrams that appear in the strong coupling expansion.

Working with a cubic lattice is equivalent to working with spin networks involving four valent vertices in the Hamiltonian approach discussed in Sec. II. In this case, it is well known that only three valent vertices have an unambiguous correspondence with the information encoded in the drawing of the spin network. Higher order vertices require additional information about the invariant tensor used to couple the irreducible representations. At the action level this means that additional group factors associated with different ways of coupling the colored surfaces at singular lines appear. In [8] this problem is dealt with by assigning colors to the singular lines which are summed over in the path integral. However, this complication may be avoided by using a special class of lattices. In the dual to a tetrahedral lattice only three plaquettes meet at each link, so singular lines involve at most three colored surfaces.

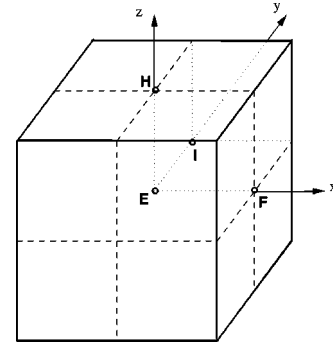


FIG. 4. Bravais unit cell.

IV. LOOP ACTIONS IN TETRAHEDRAL LATTICES

In order to introduce the tetrahedral lattice above mentioned, some concepts of solid state physics are very useful [14]. The *Bravais* lattice is one of such concepts; it specifies the periodic array in which the repeated units of a crystal are arranged. That is, the Bravais lattice summarizes the geometry of the underlying periodic structure, regardless of what the actual units are (single atoms, molecules, groups of atoms, etc.). A (three-dimensional) Bravais lattice is specified by three vectors \mathbf{a}_1 , \mathbf{a}_2 , and \mathbf{a}_3 called *primitive vectors*. The primitive vectors generate all the translations such that the lattice appears *exactly* the same. The primitive unit cell generated by the primitive vectors often does not have the full symmetry of the Bravais lattice. However, one can always consider a nonprimitive unit cell, known as a *conventional* unit cell, which is generally chosen to be bigger than the primitive cell and such that to have the full symmetry of their Bravais lattice.

Let us consider a face centered cubic Bravais lattice — i.e., the lattice obtained when one adds to the simple cubic lattice an additional point in the center of each square face — with primitive vectors $\mathbf{a}_1 = a(\mathbf{i} + \mathbf{j})$, $\mathbf{a}_2 = a(\mathbf{j} + \mathbf{k})$, $\mathbf{a}_3 = a(\mathbf{k} + \mathbf{i})$. The conventional unit cell of this lattice is a cube of side $2a$ with a four point basis located at $(0,0,0)$, $(a,0,0)$, $(0,a,0)$, $(0,0,a)$. Translations along the primitive vectors generate 27 points associated with 8 cubes of side a in the conventional cell. The Bravais conventional unit cell with the four basis points and the eight cubes is depicted in Fig. 4.

Each cube of side a may be decomposed in the five tetrahedra $ABDE$, $CBDG$, $EBGE$, $HDGE$, and $EBGD$ as shown in Fig. 5. The links of the lattice are the edges of these tetrahedra. The first four tetrahedra have volume $a^3/6$ while the last one has volume $2a^3/6$. If the vertex A of the cube depicted in Fig. 5 has coordinates $(0, -a, 0)$ the other cubes are obtained by symmetrizing with respect to the planes Exy , Eyz , Ezx and translating along the primitive vectors. Colored surfaces will be associated to the plaquettes of the dual lattice. The vertices of this lattice are the centers of the tetrahedra:

$$X_A(\epsilon) = \frac{a}{4}(\epsilon_1, 3\epsilon_2, \epsilon_3), \quad (34)$$

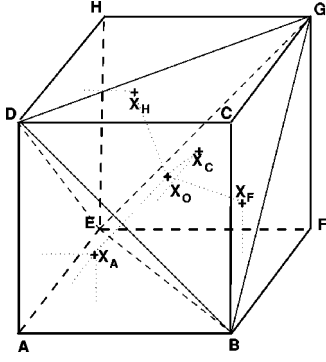


FIG. 5. Decomposition of the cube of side a in tetrahedra.

$$X_C(\epsilon) = \frac{a}{4}(3\epsilon_1, 3\epsilon_2, 3\epsilon_3), \quad (35)$$

$$X_F(\epsilon) = \frac{a}{4}(3\epsilon_1, \epsilon_2, \epsilon_3), \quad (36)$$

$$X_H(\epsilon) = \frac{a}{4}(\epsilon_1, \epsilon_2, 3\epsilon_3), \quad (37)$$

$$X_O(\epsilon) = \frac{a}{2}(\epsilon_1, \epsilon_2, \epsilon_3), \quad (38)$$

$$(39)$$

where $\epsilon = \pm 1$.

Each cell contains one polyhedron with 12 hexagonal faces and six squared faces. In Fig. 6 we show the points and links of one polyhedron and one cube. Translations along the primitive vectors fill all the lattice. Each of the squares is a face of one cube of side $a/2$. We shall attach a $SU(2)$ group element U_l in the fundamental representation to each link of this lattice.

Now let us consider the Wilson action defined in terms of the plaquettes of this lattice.

$$S = \beta \left[\sum_{p_s} \text{Re}(\text{Tr } U_{p_s}) + \sum_{p_h} \text{Re}(\text{Tr } U_{p_h}) \right], \quad (40)$$

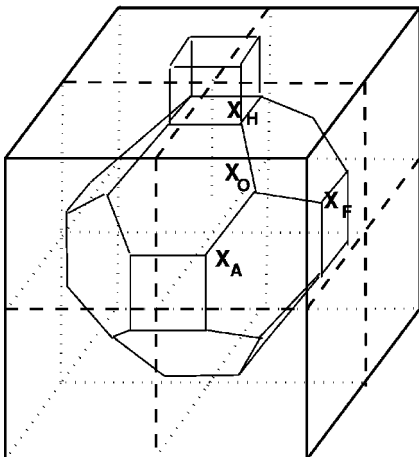


FIG. 6. Cubic and tetrahedral cells of the lattice.

where U_{p_s} and U_{p_h} respectively are the holonomies for the squared and hexagonal plaquettes.

One can show that this action has the correct continuum limit when the spacing a goes to zero, leading to the classical Yang-Mills action. This is due to the fact that the square faces as well as the hexagonal ones have equal projections over the coordinate planes. Comparing the naive continuum limit of this action with the Wilson action on a cubic lattice of side a with coupling β_c we get the following relation between the couplings: $\beta = \frac{64}{13}\beta_c$.

One can repeat the same steps leading to Eq. (31), but now the singular lines always bound three colored surfaces. In this case the integral along the boundaries in Eq. (31) only contributes when four singular lines intersect at one point and may be explicitly computed. Let us call S_k the intersecting point and $\gamma_1, \dots, \gamma_4$ the singular lines intersecting at S_k . Then we have six colored surfaces with colors $j_{12}, j_{13}, j_{14}, j_{23}, j_{24}$ and j_{34} bounded by these lines. That means that in the original tetrahedral lattice we shall have a tetrahedron with one of the values of j on each edge. The exact path integral may now be written in terms of a sum over colored surfaces:

$$Z_W = c_0^N \sum_{\text{surfaces}} \prod_i \beta_{j_i}^{A_i} (2j_i + 1)^{\epsilon_i} \times \prod_{S_k} (-1)^{\sum_i j_{ii+1}^k} \left\{ \begin{matrix} j_{12}^k & j_{13}^k & j_{14}^k \\ j_{34}^k & j_{24}^k & j_{23}^k \end{matrix} \right\}, \quad (41)$$

where the six j symbols are the Racah coefficients and the exponent of -1 denotes the cyclic sum $j_{12} + j_{23} + j_{34} + j_{41}$.

In the weak coupling limit the coefficients behave as

$$\beta_j \approx \exp \left\{ -\frac{j(j+1)}{2\beta} \right\}, \quad (42)$$

which are the coefficients of the heat kernel path integral. In what follows we will use for simplicity the heat kernel form of the partition function.

V. STRONG COUPLING EXPANSIONS

Our aim in this section is to show that the introduction of the previous Bravais lattice not only allows to perform calculations but also simplify them. Therefore, we will show here how to perform a strong coupling expansion. In order to do so we will use, just for simplicity, the expression for the path integral in terms of colored surfaces which corresponds to the heat kernel action:

$$Z = \sum_{\text{surfaces}} \prod_i \exp \left\{ -\frac{j_i(j_i+1)}{2\beta} A_i \right\} (2j_i + 1)^{\epsilon_i} \times \prod_{S_k} (-1)^{\sum_i j_{ii+1}^k} \left\{ \begin{matrix} j_{12}^k & j_{13}^k & j_{14}^k \\ j_{34}^k & j_{24}^k & j_{23}^k \end{matrix} \right\}. \quad (43)$$

We will follow an analogous treatment to that of Drouffe and Zuber [13]. We will expand in powers of the t parameter given by $t \equiv e^{-1/4\beta}$.

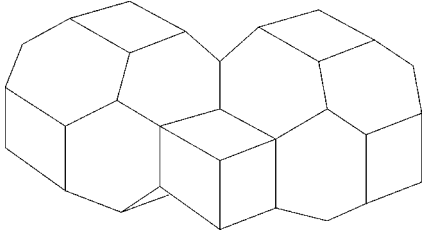


FIG. 7. First diagram involving 6-j symbols.

Free energy density f

The free energy density $f = F/N$, where $F = \log Z$ is the free energy and N the number of plaquettes, is obtained by summing the terms linear in N in the expansion of the path integral (43) in powers of t . The power of t of each diagram is equal to

$$\sum_r 2j_r(j_r+1) \times n_r,$$

where j_r denotes the representations of the group $SU(2)$ or ‘‘colors’’ and n_r denotes the number of plaquettes (square plaquettes + hexagonal plaquettes) of the diagram. For instance, the first power of the expansion corresponds to the smallest volume, i.e. the cube, with all their plaquettes with $j = \frac{1}{2}$ and it gives a power of $2 \times \frac{3}{4} \times 6 = 9$; the next power is produced by two disconnected cubes (recall that in our lattice cubes make contact only with polyhedra) with $j = \frac{1}{2}$ which gives a power of 18 and so forth. The contribution of each diagram to f can be written as the product of two numbers: the *reduced configuration number* (r.c.n.) times a group theoretical factor [13]. To compute the r.c.n. one has to count the number of inequivalent positions of a given diagram on the lattice — its *configuration number* — and then to extract the term linear in N which is the r.c.n. The group theoretical factors stem from the integrations over the link variables U_l and their general form is

$$\sum_{r \neq 0} d_r^{n_2 - n_1 + n_0} \prod_{\text{boundaries}} \chi_r(U_{\text{boundary}}),$$

where d_r is the dimension of the representation r , n_2 is the number of plaquettes with $j = j_r$, n_1 the number of distinct links bordering these plaquettes and n_0 the number of endpoints of these links. For example, diagrams with the topology of a sphere give contributions $\sum_{r \neq 0} d_r^2$. The main advantage of the introduced lattice is that the group theoretical factors for more complicated diagrams can always be explicitly expressed in terms of the d_r and 6- j Racah symbols. The Racah symbols arise each time four singular lines meet at one vertex and they appear in the diagrams by pairs. The first of this pairs come out in the diagram of two polyhedra sharing a hexagonal face and a cube sharing two of its contiguous faces, one with each polyhedron (Fig. 7).

All the external 36 plaquettes of this diagram are labeled with $j = \frac{1}{2}$ while the 3 internal (shared) plaquettes are labeled with $j = 1$; then it gives a power of $t^{3/2 \times 36 + 4 \times 3} = t^{66}$. We

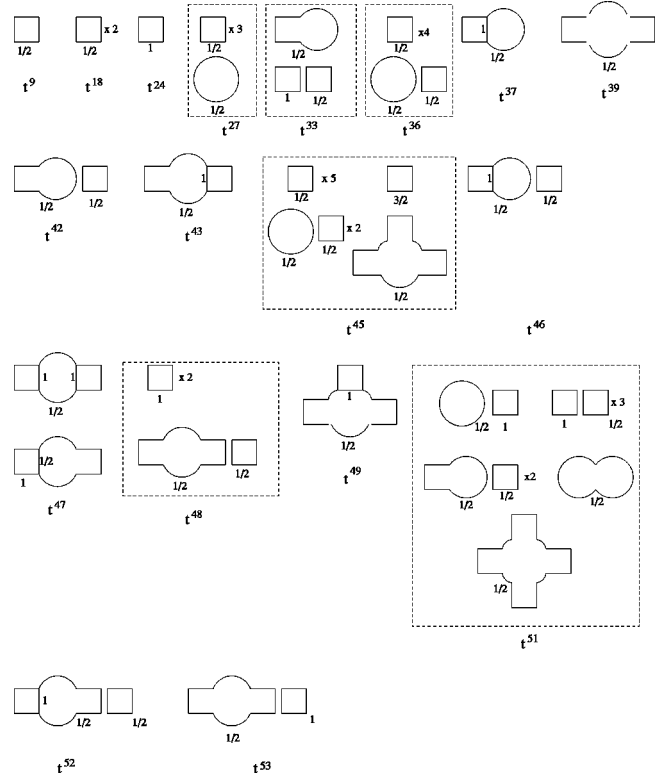


FIG. 8. Diagrams contributing to each power of t . We represent cubic cells as squares and polyhedral cells as circles. Numbers below each cell denote the representation and repeated components of a configuration are indicated by \times the multiplicity.

have computed the strong coupling expansion of f up to power 53 in t which involves 34 diagrams grouped in 18 different powers of t :

$$\begin{aligned} f = & 4t^9 - 8t^{18} + 9t^{24} + 76/3t^{27} - 12t^{33} - 160t^{36} + 72t^{37} \\ & + 60t^{39} - 432t^{42} + 360t^{43} + 8224/5t^{45} + 612t^{46} - 1728t^{47} \\ & - 2961/2t^{48} + 720t^{49} + 5052t^{51} - 8640t^{52} + 2664t^{53}. \end{aligned} \quad (44)$$

In Fig. 8 we list schematically the diagrams contributing to each power of t .

We plot in Fig. 9 the f vs β for different powers of truncation of the expansion and the series expansion for a cubic lattice of Ref. [13]. We observe the coincidence of both expansions up to $\beta = 0.5$.

As long as we enter in the weak coupling regime ($\beta > 1$), one can appreciate a clear difference with the series expansions of Ref. [13] which were performed in an ordinary cubic lattice and with a different truncation criteria (they consider diagrams up to 16 plaquettes which corresponds to t^{24}). Our series seems to be more consistent with the expected linear behavior in the weak coupling limit. The explanation of this difference relies on the fact that in the strong coupling expansion in a cubic lattice up to 16 plaquettes all the terms except two are positive while in our case we have almost equal number of contributions with both signs.

Thus, one can observe that the introduction of the dual of the tetrahedral lattice, besides simplifying the strong cou-

Free energy density.

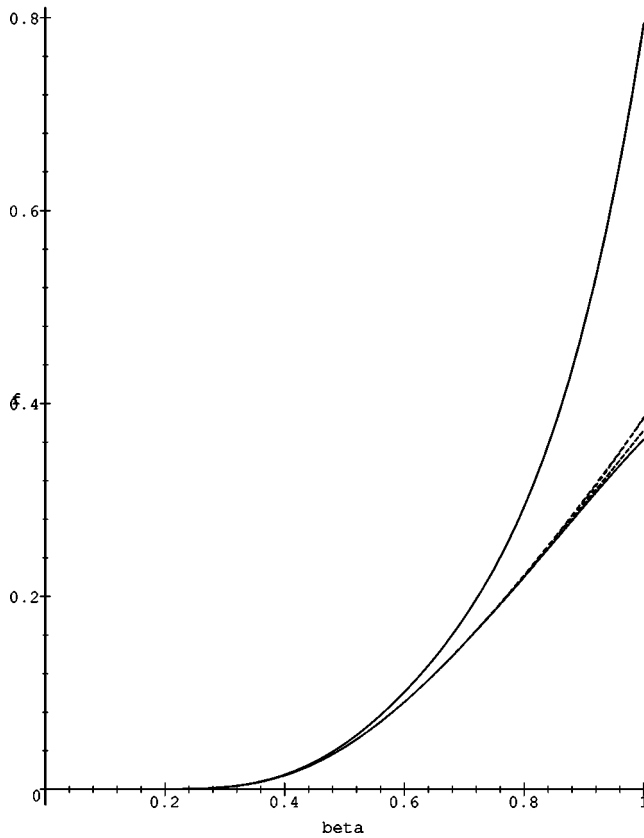


FIG. 9. Free energy f vs β for several truncation orders. From above: t^{27} , t^{39} , t^{46} , t^{53} and t^{18} .

pling computations provides a straightforward procedure to obtain the desired terms of the series expansion. This turns to be an advantage in order to reach the weak coupling regime.

VI. CONCLUSIONS

We have introduced a Hamiltonian spin network representation for a $SU(2)$ lattice gauge theory. This gauge invariant representation is given in terms of an independent basis that diagonalizes the electric part of the Hamiltonian. The corresponding Lagrangian formulation is also developed.

This formulation takes a purely geometrical form in terms of sums over colored surfaces and allows to combine the powerful Lagrangian techniques with the redundancy free description typical of the loop representation. This action may be written on a tetrahedral lattice explicitly in terms of the Racah coefficients. The computation of the group theoretical factors of the strong coupling expansion becomes straightforward, only involving these Racah coefficients. Also, we have a compact expression for the colored surfaces action which allows to perform numerical computations.

In the naive weak coupling limit, the area dependent factors become equal to 1 and the action is purely topological. One can immediately check that this limit corresponds to the Ouguri [15] form of the B-F topological field theory, which in three dimensions is known [16] to coincide with the pure gravity action. This rather unexpected result may be understood if one recalls that the action of the Yang-Mills theory in three dimensions may be written in terms of a one-form B and the field strength F as follows: $S = \int B \wedge F - g^2 B \wedge *B$ and therefore for g going to 0 it reduces to the three dimensional B-F theory. This provides an explicit proof of the relation between the B-F theory and the Ouguri-Turaev-Viro sum over colored surfaces [17]. In this case the use of the Biedenharn and Elliot identity [18] allows us to show that the action is invariant under the renormalization group. Thus, in the different context of QCD, this suggests that the Yang-Mills action in terms of colored surfaces may be particularly well suited for the study of the effective theories.

Even though the method developed here was for $SU(2)$ in 2+1 dimensions, the extension to other groups, in particular to $SU(3)$, is straightforward. The corresponding spin networks would simply carry the quantum numbers required to characterize the irreducible representations of the Lie group under study [19]. It is also possible to extend this formulation to the four dimensional case, by making use of the higher order Racah-Wigner j -coefficients. An important simplification of the path integral (43) with the same weak coupling regime could be obtained by making use of the Ponzano and Regge asymptotic form of the Racah-Wigner j -symbols. We hope to present elsewhere a more detailed analysis of these developments.

ACKNOWLEDGMENTS

This work has been supported in part by the CIRIT project ACI014.

-
- [1] R. Gambini and A. Trias, Phys. Rev. D **22**, 1380 (1980).
 - [2] R. Gambini and A. Trias, Nucl. Phys. **B278**, 436 (1986).
 - [3] A. Ashtekar, Phys. Rev. Lett. **57**, 2244 (1986); Phys. Rev. D **36**, 1587 (1987).
 - [4] C. Rovelli and L. Smolin, Phys. Rev. Lett. **61**, 1155 (1988); Nucl. Phys. **B331**, 80 (1990).
 - [5] J. M. Aroca, M. Baig, and H. Fort, Phys. Lett. B **336**, 54 (1994).
 - [6] J. M. Aroca, M. Baig, H. Fort, and R. Siri, Phys. Lett. B **366**, 416 (1995).
 - [7] C. Rovelli and L. Smolin, Phys. Rev. D **52**, 5743 (1995); L. P. Hughston and R. S. Ward, *Advances in Twistor Theory* (Pitman, New York, 1979).
 - [8] M. Reisenberger, gr-qc/9412035, 1994.
 - [9] J. M. Aroca, H. Fort, and R. Gambini, Phys. Rev. D **54**, 7751 (1996).
 - [10] C. Itzykson and J. M. Drouffe, in *Statistical Field Theory* (Cambridge University Press, Cambridge, England, 1989), Vol. 1
 - [11] L. Kauffman and S. Lins, *Temperley-Lieb Recoupling Theory*

- and Invariants of 3-Manifolds* (Princeton University Press, Princeton, NJ, 1994).
- [12] D. Robson and D. M. Webber, *Z. Phys. C* **15**, 199 (1982); A. C. Irving, T. E. Preece, and C. J. Hamer, *Nucl. Phys.* **B270**, 536 (1986); C. J. Hamer, A. C. Irving, and T. E. Preece, *ibid.* **B270**, 553 (1986).
- [13] J. M. Drouffe and J. B. Zuber, *Phys. Rep.* **102**, 1 (1983), and references therein.
- [14] N. W. Ashcroft and N.D. Mermin, *Solid State Physics* (Saunders College Publishing, Philadelphia, 1976).
- [15] H. Ouguri, *Nucl. Phys.* **B382**, 276 (1992).
- [16] E. Witten, *Commun. Math. Phys.* **181**, 351 (1989).
- [17] V. G. Turaev and O. Viro, *Topology* **31**, 865 (1992).
- [18] L. C. Biedenharn, *J. Math. Phys.* **31**, 287 (1953).
- [19] S. P. Martin, *Nucl. Phys.* **B338**, 244 (1990).